



Combining two optimized and affordable methods to assign chemoreceptors to a specific signal

Anne Boyeldieu, Amine Ali Chaouche, Vincent Méjean, Cécile Jourlin-Castelli

► To cite this version:

Anne Boyeldieu, Amine Ali Chaouche, Vincent Méjean, Cécile Jourlin-Castelli. Combining two optimized and affordable methods to assign chemoreceptors to a specific signal. *Analytical Biochemistry*, 2021, 620, pp.114139. 10.1016/j.ab.2021.114139 . hal-03195889

HAL Id: hal-03195889

<https://hal.science/hal-03195889>

Submitted on 10 Mar 2023

HAL is a multi-disciplinary open access archive for the deposit and dissemination of scientific research documents, whether they are published or not. The documents may come from teaching and research institutions in France or abroad, or from public or private research centers.

L'archive ouverte pluridisciplinaire **HAL**, est destinée au dépôt et à la diffusion de documents scientifiques de niveau recherche, publiés ou non, émanant des établissements d'enseignement et de recherche français ou étrangers, des laboratoires publics ou privés.



Distributed under a Creative Commons Attribution - NonCommercial 4.0 International License

Combining two optimized and affordable methods to assign chemoreceptor(s) to a specific signal

Anne Boyeldieu^a, Amine Ali Chaouche^a, Vincent Méjean^a, Cécile Jourlin-Castelli^{a*}

Short title: Assigning chemoreceptor(s) to a ligand

^aAix Marseille Univ, CNRS, BIP UMR 7281, IMM, IM2B, Marseille, France

*Corresponding author

Mailing address: Laboratoire de Bioénergétique et Ingénierie des Protéines (BIP-UMR7281), Institut de Microbiologie de la Méditerranée, Centre National de la Recherche Scientifique, 31 chemin Joseph Aiguier, CS 70071, 13402 Marseille cedex 09, France

Tel: 33 4 91 16 40 32

Fax: 33 4 91 16 40 97

E-mail: jourlin@imm.cnrs.fr

Subject Category : Special Topics

Abstract

Chemotaxis allows bacteria to detect specific compounds and move accordingly. This pathway involves signal detection by chemoreceptors (MCPs). Attributing a chemoreceptor to a ligand is difficult because there is a lot of redundancy in the MCPs that recognize a single ligand. We propose a methodology to define which chemoreceptors bind a given ligand. First, an MCP is overproduced to increase sensitivity to the ligand(s) it recognizes, thus promoting accumulation of cells around an agarose plug containing a low attractant concentration. Second, the ligand-binding domain (LBD) of the chemoreceptor is fused to maltose-binding protein (MBP), which facilitates purification and provides a control for a thermal shift assay (TSA). An increase in the melting temperature of the LBD in the presence of the ligand indicates that the chemoreceptor directly binds it. We showed that overexpression of two *Shewanella oneidensis* chemoreceptors (SO_0987 and SO_1056) promoted swimming toward an agarose plug containing a low concentration of chromate. The LBD of each of the two chemoreceptors was fused to MBP. A TSA revealed that only the LBD from SO_1056 had its melting temperature increased by chromate. In conclusion, we describe an efficient approach to define chemoreceptor-ligand pairs before undertaking more-sophisticated biochemical and structural studies.

Keywords: Bacterial chemotaxis; Signal detection; Methyl-accepting Chemotaxis Protein; Thermal Shift Assay; Agarose-in-plug bridge assay; MBP chimeric proteins.

39 1. Introduction

40 Bacteria encounter changing environments to which they adapt via a variety of mechanisms. In
41 addition to adaptation through the regulation of gene expression, bacteria also control their movement
42 within their environment using a mechanism called chemotaxis [1,2]. Upon detection of signal
43 molecules called chemoeffectors, cells modulate their swimming behavior to move toward attractants
44 or away from repellents. Chemotaxis is governed by a complex regulatory system composed of various
45 Che proteins [3]. The well-conserved CheA-CheY histidine-kinase/response-regulator pair, which
46 engage in a phosphorylation cascade, directly controls the rotational direction of the flagellum, which
47 propels the bacterium. The first step in chemotaxis is the detection of chemoeffectors by specific
48 chemoreceptor proteins called MCPs (Methyl-accepting Chemotaxis Proteins) [2,4]. The binding of
49 chemoeffectors to MCPs then affects the phosphorylation cascade involving CheA-CheY, and
50 consequently, bacterial movement.

51 Bacterial genomic analysis has revealed a large number of MCP-encoding genes, with some bacteria
52 containing more than 80 [5]. Chemoreceptors are characterized by the presence of a highly conserved
53 signaling domain within their cytoplasmic region. However, they also contain additional domains.
54 Chemoreceptors can be classified according to the number of helical heptads that are contained within
55 their signaling domain [5,6]. They can also be classified based on their topologies and the type of
56 ligand-binding domain (LBD) they contain [4,7]. Cache, 4HB and PAS-containing domains are among
57 the most common types of LBDs. The first described Cache domains were involved in small-molecule
58 recognition [8]. Today, a large superfamily of different types of single and double Cache domains has
59 been documented, and some ligands, such as amino acids, polyamines, carboxylic acids, sugars and
60 hydrocarbons have been identified [9–11]. The 4HB (four-helix bundle) domain, which is widespread
61 in signal transduction systems, has been shown to bind ligands such as amino, aromatic and carboxylic
62 acids directly [10,12]. PAS domains, which are exclusively present in the cytoplasm, allow signal
63 detection via direct binding to small molecules, including divalent cations or carboxylic acids. PAS-
64 domain interactions can also be mediated by the presence of cofactors (heme b or c, FAD, FMN) for
65 detection of signals such as oxygen or redox potential [13].

66 *Escherichia coli*, which has been a model for bacterial chemotaxis for many years, possesses only five
67 chemoreceptors, all of which have been well characterized [14]. Four *E. coli* chemoreceptors contain
68 a 4HB domain (Tar, Tsr, Trg and Tap), while one possesses a FAD-containing PAS domain (Aer). *E.*
69 *coli* is able to respond chemotactically to various signals, including amino acids, sugars, dipeptides,
70 quorum-sensing signals, pH and redox potential. Some signals are directly detected by the
71 chemoreceptors, while the detection of others requires auxiliary proteins. For example, the Tar

72 chemoreceptor detects aspartate by direct binding to the Tar LBD and recognizes maltose via the
73 maltose-binding protein (MBP).

74 Many bacteria have far more chemoreceptors than *E. coli*, especially bacteria that typically encounter
75 changing environmental conditions [15]. For example, several species of the *Pseudomonas* genus
76 contain more than 20 chemoreceptors. Aside from classical ligands (amino acids, carboxylic acids,
77 sugars), some Pseudomonads use specific chemoreceptors to detect atypical molecules such as toluene,
78 aromatic hydrocarbons and naphthalene [16]. *Shewanella oneidensis*, an aquatic bacterium, possesses
79 27 chemoreceptors. It is chemotactically attracted to various respiratory substrates (oxygen, nitrate,
80 fumarate, TMAO), but, more surprisingly, it is also attracted to chromate, a toxic compound [17–19].
81 While five chemoreceptors have been shown to be involved in responses to respiratory substrates [18],
82 the chemoreceptor(s) responsible for detecting chromate remain(s) unknown.

83 Despite the fact that the number of characterized LBDs has increased over last few years, it remains
84 challenging to assign a ligand to a chemoreceptor, and vice versa. This is especially true because MCPs
85 containing LBDs of the same type may detect many different ligands. Additionally, the same ligand
86 may be detected by MCPs with different types of LBD. One strategy corresponds to the
87 characterization of chemoreceptors one by one, testing their capacity to bind molecules from various
88 libraries *in vitro* [20,21]. This strategy allows the identification of one or several compounds capable
89 of binding a chemoreceptor. However, compounds identified in this way are not necessarily
90 chemoeffectors, since the method does not assess their capacity to elicit a chemotactic response.
91 Nevertheless, this strategy can be helpful when no chemoeffector has been identified within the
92 organism studied, since the identification of chemoreceptor ligands has the potential to inform about
93 the nature of compounds to which an organism may respond. However, a chemoeffector detected by a
94 specific chemoreceptor can be missed using this strategy, because many chemoreceptors detect signals
95 indirectly, for instance via interactions with periplasmic ligand-binding proteins.

96 Use of a different strategy based on gene deletions is possible when compounds are known to elicit
97 chemotactic behavior for a given bacterium since, in this scenario, one must determine which
98 chemoreceptor(s) is involved in the detection of a specific compound [22]. As mentioned above, this
99 too may be complicated by the fact that bacteria usually possess many chemoreceptors and more than
100 one chemoreceptor is often capable of detecting the same ligand. Here, we propose an easy and
101 inexpensive strategy combining optimized versions of *in vivo* and *in vitro* experiments to determine
102 which chemoreceptor(s) is/are involved in the direct recognition of a ligand via their LBD.

103

2. Materials and Methods

2.1 Strains.

The wild-type *S. oneidensis* strain used in this study was MR1-R [23]. All strains were routinely grown at 28°C (*S. oneidensis* strains) or 37°C (*E. coli* strains) in lysogeny broth (LB) medium. When necessary, chloramphenicol (25 µg/ml), rifampicin (10 µg/ml) or ampicillin (50 µg/ml) was added. The concentration of arabinose used for inducing expression of plasmid-borne genes was 0.2%.

2.2 Construction of double-deletion mutant.

The ΔSO0987ΔSO1056 mutant strain was constructed by sequential deletion of the *so_0987* and *so_1056* genes from the genome of the wild-type strain. This deletion mutant was constructed by homologous recombination as described previously [18]. Briefly, 500 bp flanking regions downstream and upstream of the gene to be deleted were cloned into the suicide vector pKNG101. The resulting plasmid was introduced into the *E. coli* strain CC118λpir [24] and transferred into the appropriate *S. oneidensis* strain by conjugation using the *E. coli* helper strain 1047/pRK2013 [25]. The plasmid was integrated into the chromosome by a first recombination event and removed by a second recombination event in the presence of 6% sucrose. Deletions were confirmed using PCR and appropriate primers.

2.3 Construction of plasmids.

All plasmids used in this study are listed in Table 1. To construct pSO0987, pSO1056, pSO2240, pSO3282, pSO4053, pSO4454 and pSO4557, the coding sequences of the respective genes were amplified by PCR using *S. oneidensis* DNA as a template and primers containing appropriate restriction sites and an optimized Shine Dalgarno sequence. After digestion, PCR products were inserted into the pBAD33 vector. To construct pMAL-LBD-0987 and pMal-LBD-1056, the sequences encoding the LBD of SO_0987 (Y30 to S200) and SO_1056 (S29 to M278) were amplified by PCR using *S. oneidensis* DNA as a template and primers containing appropriate restriction sites. After digestion, PCR products were inserted into the pMAL-c2X vector. The sequences of all constructs were confirmed via DNA sequencing using appropriate primers.

133 **Table 1**

134 Plasmids used in this study

Plasmids	Descriptions	References
pBAD33	Vector containing pBAD promoter with the p15A origin of replication, Cm ^R	[26]
pSO0987	<i>so_0987</i> sequence cloned into pBAD33	This work
pSO1056	<i>so_1056</i> sequence cloned into pBAD33	This work
pSO2240	<i>so_2240</i> sequence cloned into pBAD33	This work
pSO3282	<i>so_3282</i> sequence cloned into pBAD33	This work
pSO4053	<i>so_4053</i> sequence cloned into pBAD33	This work
pSO4454	<i>so_4454</i> sequence cloned into pBAD33	This work
pSO4557	<i>so_4557</i> sequence cloned into pBAD33	This work
pMAL-c2X	Vector containing <i>ptac</i> promoter and the coding sequence of MBP, Amp ^R	New England Biolabs
pMAL-LBD-0987	Sequence coding for the ligand-binding domain of SO_0987 (Y30 to S200) cloned into pMAL-c2X	This work
pMAL-LBD-1056	Sequence coding for the ligand-binding domain of SO_1056 (S29 to M278) cloned into pMAL-c2X	This work
pKNG101	R6K-derived suicide plasmid containing Str ^R and <i>sacB</i>	[24]
pRK2013	RK2-Tra1 RK2-Mob1 Kan ^R <i>ori</i> ColE1	[25]

135

136

137

138 **2.4 Agarose-in-plug bridge assays.**

139 *2.4.1 Construction of bridge slide.* Microscope bridge slides were constructed as described previously
140 [27]. Briefly, two square coverslips were placed on each side of a PETG slide. Four to eight agarose
141 plugs per slide were made by pipetting 5µl preheated 2% low-melting agarose that contained the
142 chemical to be tested onto the slide. Within a few seconds, a glass coverslip (24 mm × 60 mm) was
143 placed over the slide. The bridge structure is maintained using a cyanoacrylate adhesive.

144

145 *2.4.2 Cell preparation and microscopic observation.* Cells were prepared as described in Armitano et
146 al. [27], with slight modifications. Briefly, cells were grown overnight in LB medium under shaking
147 conditions at 28°C. Cells were subsequently diluted in fresh LB medium at an OD₆₀₀ value of 0.05 and
148 grown under shaking conditions until an OD₆₀₀ value of 0.7-0.8 was reached. Cells were then harvested
149 by centrifugation (10 min at 3,500 rpm) and gently resuspended in LM medium (0.2 g/l yeast extract,
150 0.1 g/l peptone, 10 mM HEPES (pH 7.4) and 10 mM NaHCO₃) containing 20 mM lactate and 0.1%
151 Tween-20 to produce an OD₆₀₀ of 0.2. After 30 min of static incubation at room temperature, 150 µL
152 of cell suspension was introduced within the microscope slide bridge. Photographs were taken at the
153 edges of the plugs after 30 min with a 4X phase contrast objective. Strains containing pBAD33,
154 pSO0987, pSO1056, pSO2240, pSO3282, pSO4053, pSO4454 or pSO4557 were grown overnight in
155 the presence of chloramphenicol, and arabinose was subsequently added to induce gene expression.

156

157 **2.5 Expression and purification of MBP-LBD chimeric proteins.**

158 Recombinant MBP-tagged proteins, MBP-LBD₀₉₈₇ and MBP-LBD₁₀₅₆, were produced from the *E. coli*
159 C600 strain [28] that contained a pMAL-LBD-0987 or pMAL-LBD-1056 plasmid, respectively. The
160 strains were grown aerobically at 37°C in LB medium. At OD₆₀₀ = 0.5, overproduction of proteins was
161 induced with 0.3 mM isopropyl β-D-thiogalactopyranoside (IPTG). After 3 h at 37°C, cells were
162 collected by centrifugation and resuspended in 20 mM Tris-HCl (pH 7.4), 200 mM NaCl, and 1 mM
163 EDTA. Thereafter, they were lysed using a French press and centrifuged at 11,000 rpm for 20 min at
164 4°C. After an ultracentrifugation step at 45,000 rpm for 1 h at 4°C, the supernatant was loaded onto an
165 amylose high-flow resin (New England Biolabs), and proteins were purified according to the
166 manufacturer's protocol. Purified proteins were loaded onto a PD-10 desalting column (GE
167 Healthcare) and recovered in 20 mM Tris-HCl (pH 7.4) containing 100 mM NaCl. Protein

168 concentrations were determined using a Bradford assay (Bio-Rad). Purified proteins were store at
169 - 80°C in 20 mM Tris-HCl (pH 7.4), 100 mM NaCl and 10% glycerol.

170

171 **2.6 Thermal shift assays.**

172 TSAs were carried out using purified proteins in 20 mM Tris-HCl (pH 7.4), 100 mM NaCl and 10 %
173 glycerol in a total volume of 20 µL, as described previously [29]. Briefly, either MBP-LBD₀₉₈₇ (11.2
174 µM) or MBP-LBD₁₀₅₆ (7.8 µM) was incubated in the presence of 10X SYPRO Orange (Sigma Life
175 Science) with or without potassium chromate (1 mM and 10 mM) and maltose (10 mM). Samples were
176 then heated from 10 to 90°C at a scan rate of 0.5°C per 30 s using a BioRad CFX96 Touch Real Time
177 PCR instrument. Protein unfolding curves were monitored by detecting changes in SYPRO Orange
178 fluorescence. Melting temperatures were determined from first derivative values of raw fluorescence
179 data using BioRad CFX Manager 3.1 software.

180

181 **3. Results and Discussion**

182 **3.1 Scientific rationale of the experimental strategy.**

183 Various techniques have been described to test the chemotactic abilities of bacteria. Among these, the
184 agarose-in-plug bridge assay has been successfully used to study the behavior of different bacterial
185 species [16,27,30–34]. Using this approach, the chemical to be tested is included in an agarose drop
186 and placed on a microscope slide. A bacterial suspension is then injected in the area surrounding the
187 agarose. If the chemical is an attractant, its diffusion into the bacterial suspension will cause cells to
188 move toward the plug, which produces a microscopically observable bright ring of cells. One can then
189 compare the behavior of a wild-type strain to that of mutants that harbor an MCP-deletion.

190 However, because signal-detection redundancy occurs, in which several MCPs bind the same ligand,
191 the behavior of a single MCP-deletion mutant may not be distinguishable from that of its wild-type
192 counterpart. Moreover, a gene-deletion analysis is not an easy task for bacteria that contain many
193 chemoreceptor-encoding genes. To overcome this pitfall, we propose the use of a reverse
194 methodology. Using this experimental rationale, instead of deleting an MCP-encoding gene in order
195 to observe a reduced chemotactic response after exposure to a specific ligand, we propose cloning and
196 overexpressing MCP-encoding genes in a wild-type strain. As the relative expression level of a
197 chemoreceptor defines the sensitivity of response it mediates [35], the capacity of the resulting strains

198 to detect and respond to a concentration below that to which a control strain containing an empty vector
199 is able to respond will be checked (Fig. 1A and B).

200 The chemoreceptor(s) identified by this approach will be tested *in vitro* using a simple thermal shift
201 assay (TSA) to determine whether or not the detection of chemoattractant occurs via direct binding of
202 the ligand to the chemoreceptor(s). Since the heterologous expression of entire chemoreceptors or of
203 their LBDs in *Escherichia coli* could result in the formation of insoluble proteins that form inclusion
204 bodies [36], we suggest that LBDs should be produced as chimeric proteins fused to MBP. Fusion to
205 MBP has previously been shown to facilitate the solubilization of proteins that otherwise formed
206 inclusion bodies (Fig. 1C) [37,38]. This strategy is an alternative to the recovery of proteins from
207 inclusion bodies, which requires subsequently refolding and purification [36]. Interaction between a
208 chimeric protein and ligand can then be assessed using a TSA [39]. This rapid and inexpensive
209 technique is easy to set up and requires only a thermocycler, which is commonly found in microbiology
210 laboratories. Moreover, it requires only low concentrations of proteins and can be performed in 96-
211 well microplates, unlike isothermal titration calorimetry (ITC), which is a direct binding test
212 commonly used to confirm ligand-protein interactions.

213 TSA requires proteins to be subjected to thermal denaturation in the presence of a dye (SYPRO
214 Orange), which is fluorescently active when bound to hydrophobic domains of proteins exposed by
215 thermal unfolding. Usually, ligand binding to a protein increases its thermal stability, which produces
216 a detectable shift to a higher melting temperature (Fig. 1D). Moreover, TSA was previously proved to
217 be a suitable technique for ligand-chemoreceptor interaction screening [20,21,40,41]. Adding MBP to
218 form a chimeric protein provides an additional advantage, since MBP is able to function as an internal
219 control whose denaturation profile should only be affected by maltose, its natural ligand. Below, we
220 describe how this combined strategy was used to characterize chemoreceptor(s) involved in the
221 detection of chromate, an attractant peculiar to *S. oneidensis*.

222

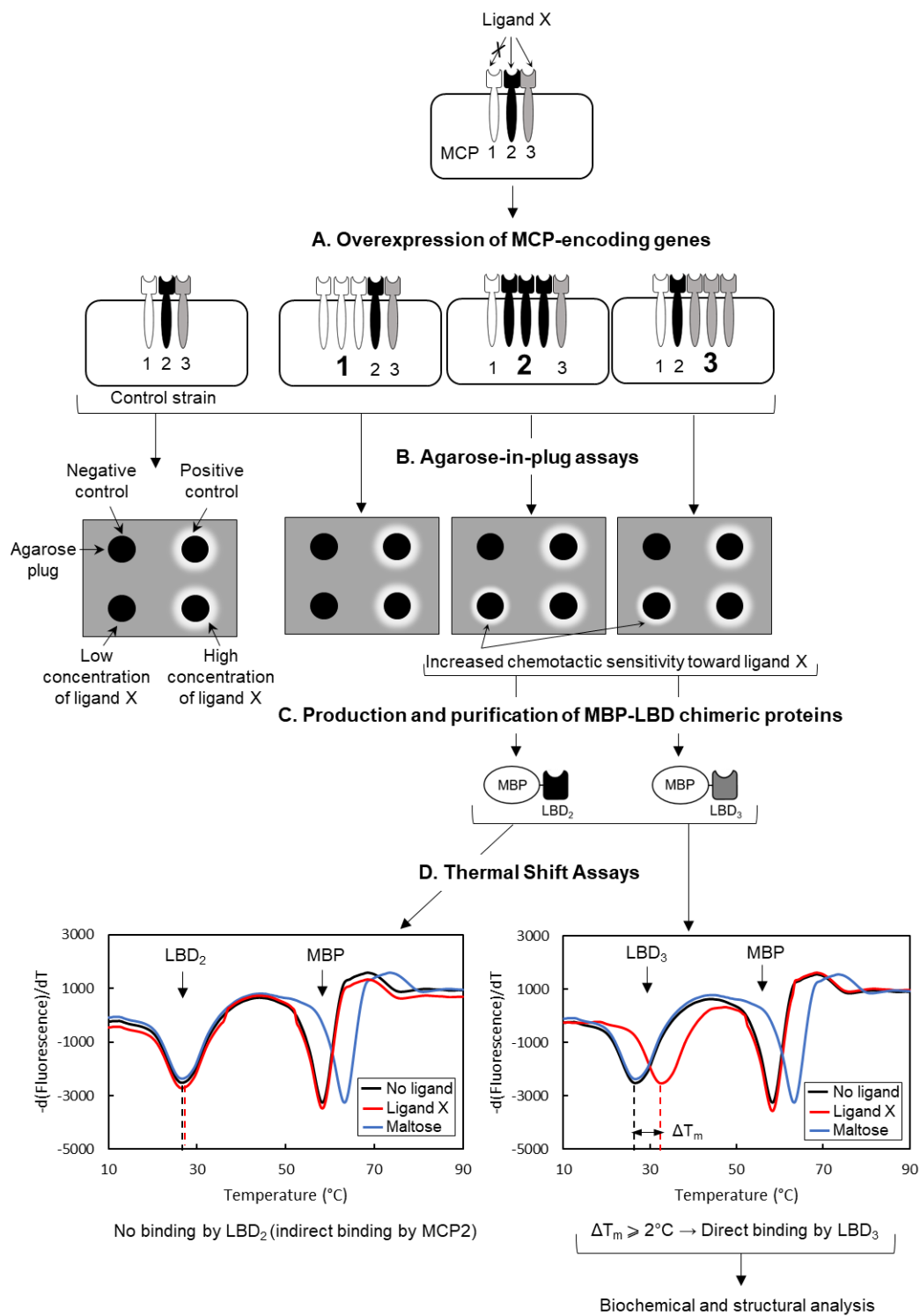


Figure 1. A scheme outlining the strategy used to identify chemoreceptors (MCPs) involved in specific ligand recognition. A) Each gene encoding an MCP to be tested was overexpressed in a wild-type background. B) Agarose-in plug assays were used to test the chemotactic behavior of each MCP-overexpressing strain toward ligand X. MCPs whose overproduction enhances the chemotactic sensitivity of the wild-type strain, as indicated by a bright ring of cells around a plug containing a low concentration of ligand X, are selected as candidates for ligand X recognition. C) The ligand-binding domains (LBD) of the selected MCPs are fused to maltose-binding protein (MBP). The resulting MBP-LBD fusions are overproduced and purified, taking advantage of the ability of MBP to bind to amylose. D) Interactions between MBP-LBD

fusions and ligand X are tested using TSA. Curves of the first derivative of fluorescence emission with respect to temperature should contain two negative peaks that corresponded either to the MBP or LBD moiety of each chimeric protein. Maltose is used to identify the peak that corresponds to MBP. The two peaks allow us to determine the melting temperature (T_m) of each moiety of the chimeric protein in the absence and presence of ligand X. When the addition of ligand X does not modify the T_m of the LBD, ligand X probably does not bind directly to the LBD. A T_m shift for the LBD in the presence of ligand X ($\Delta T_m \geq 2^\circ\text{C}$) indicates that the LBD binds ligand X directly. The LBD-ligand X interaction can then be further characterized with other methods.

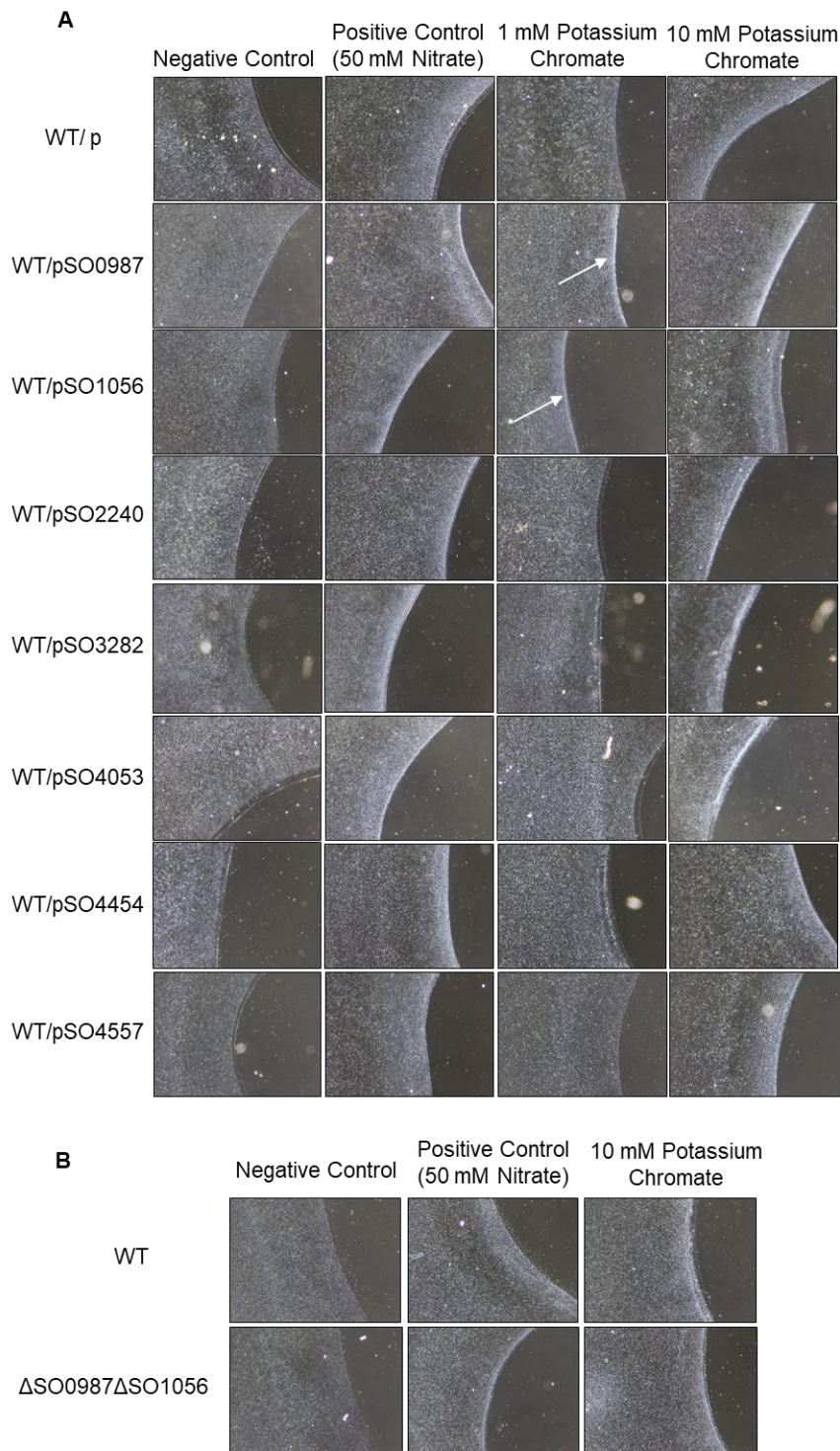
3.2 Combining the overexpression of chemoreceptor-encoding genes with an agarose-in-plug bridge assay enabled the identification of two chemoreceptors involved in the chemotactic response to chromate.

S. oneidensis is attracted to chromate, a toxic metal to which it is resistant [19]. To the best of our knowledge, this is the only example of bacterial chemotaxis toward chromate. Therefore, no specific motif for chromate binding has been previously described. Recently, we described an efflux pump, ChrA_{SO}, involved in *S. oneidensis* chromate resistance [42]. A gene (*so_0987*) encoding a chemoreceptor was identified immediately downstream and in the same orientation as the *chrA_{SO}* (*so_0986*) gene. Apart from its location, the *so_0987* gene drew our attention because it encodes a chemoreceptor with a Cache domain in its LBD. Since Cache domains are capable of binding small molecules, we decided to test not only SO_0987 but also other Cache-containing chemoreceptors for their ability to detect chromate [8]. The *S. oneidensis* genome is predicted to encode the following Cache-domain containing chemoreceptors: SO_0987 and SO_2240 (sCache2); SO_1056, SO_1278, SO_4454, SO_4557 and SO_4466 (dCache1); SO_4053 (dCache3) and SO_3282 (Cache3-Cache2) [5]. Except for SO_1278 and SO_4466, which were associated with lowest Cache domain prediction E-values, all genes encoding Cache-containing chemoreceptors were independently cloned under the control of an arabinose-inducible promoter. The resulting plasmids were introduced into the wild-type *S. oneidensis* reference strain (MR1-R), and chemotactic behaviors of the strains were tested via the agarose-in-plug bridge assay.

As shown in Figure 2A, the wild-type strain that contained an empty vector was attracted to nitrate (used as a control) and also to chromate when it was present at 10 mM in the plug, as indicated by the presence of a bright ring of cells close to the plug. However, when only 1 mM chromate was added to the plug, it did not attract wild-type bacteria. Among the seven chemoreceptor genes tested, the overexpression of only two (*so_0987* and *so_1056*) resulted in a bright ring of cells around the plug containing 1 mM chromate; attraction to nitrate remained unchanged (Fig. 2A). These results indicate

264 that the cells overexpressing either *so_0987* or *so_1056* are attracted to chromate with a higher
 265 sensitivity than the control strain.

266 In addition to these two chemoreceptors, likely others are also involved in the detection of chromate,
 267 as a strain containing deletions of *so_0987* and *so_1056* was still attracted to chromate (Fig. 2B).



268

269 **Figure 2. Agarose-in-plug bridge assays to identify dedicated chemoreceptors.** A) Agarose-in-plug bridge assays of a
 270 wild-type (WT) *S. oneidensis* strain containing either an empty vector (p) or one of the seven plasmids bearing Cache-

271 containing MCP-encoding genes (pSO0987, pSO1056, pSO2240, pSO3282, pSO4053, pSO4454 or pSO4557) are shown.
272 B) Agarose-in-plug bridge assays of wild-type (WT) and Δ SO0987 Δ SO1056 strains are shown. Cells were grown in LB
273 containing 0.2% arabinose under shaking conditions until an OD₆₀₀ of 0.7-0.8 was reached. Cells were then harvested by
274 centrifugation and resuspended in LM medium containing lactate and Tween-20. The chemotactic behaviors of the strains
275 toward a plug that contained either water (negative control), 50 mM sodium nitrate (positive control), or 1 mM or 10 mM
276 potassium chromate were tested using an agarose-in-plug bridge assay. Photographs were taken at the edges of the plug
277 after 30 min of incubation (4× magnification). White arrows indicate the accumulation of cells around a plug containing a
278 low concentration of potassium chromate (A). All pictures are representative of three independent experiments.

279

280 3.3 The LBD of one of the two identified chemoreceptors directly binds chromate.

281 To test whether the detection of chromate by the two chemoreceptors is direct, we performed TSAs
282 using purified proteins. The SO_0987 and SO_1056 proteins are predicted to share a similar topology,
283 with two transmembrane segments delimiting the LBD. Each LBD is predicted to be periplasmic and
284 contains a Cache domain. Therefore, we cloned the region encoding the LBD of each chemoreceptor
285 in frame with an MBP-encoding gene. The gene fusions were placed under the control of the IPTG-
286 inducible *ptac* promoter, which allowed their overexpression. The two chimeric MBP-LBD proteins
287 proved to be soluble when overproduced. Overproduction of the corresponding Strep-tagged LBDs
288 resulted in insoluble proteins that were found in inclusion bodies.

289 The two chimeric MBP-LBD proteins were subsequently purified using an amylose resin column. The
290 two purified proteins were then submitted to thermal denaturation in the presence of SYPRO Orange
291 fluorescent dye. To determine the melting temperature (T_m), the first derivatives of melt curves are
292 shown (Fig. 3). Similar curves displaying two peaks were observed for each chimeric protein in the
293 absence of ligand (Fig. 3A and B; black curves). We assumed that each moiety of the chimeric protein
294 is capable of folding independently, and thus reacts differently to thermal denaturation.

295 To assign each peak to a specific moiety of the chimeric protein, we submitted the MBP-LBD₀₉₈₇
296 protein to thermal denaturation in the presence of maltose, the ligand of MBP. Only the second peak
297 of the melt curve of the chimeric protein shifted in response to the presence of maltose, indicating that
298 this peak corresponded to the MBP moiety (Fig. 3A, blue curve). This strongly suggested that the first
299 peak was associated with the LBD moiety of the chimeric protein.

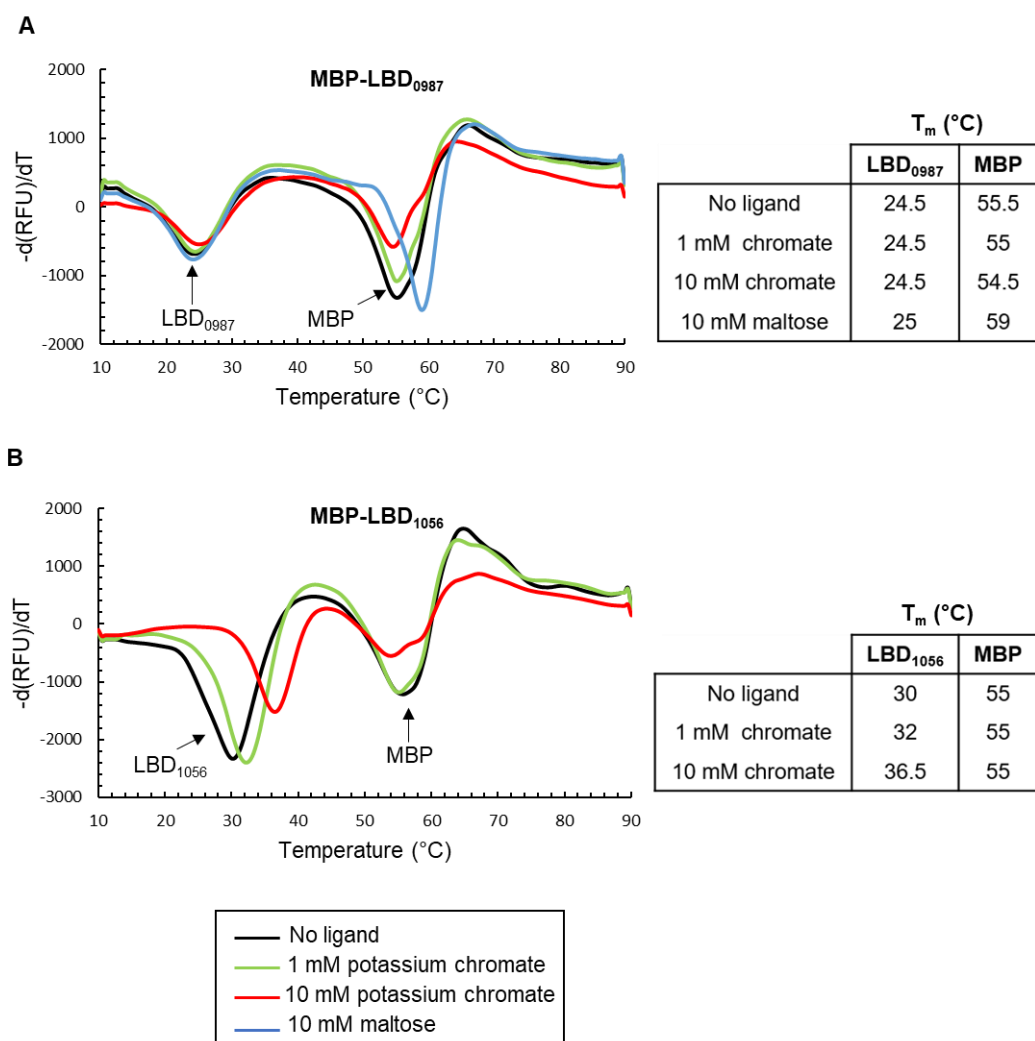


Figure 3. Thermal shift assays with MBP-LBD₀₉₈₇ and MBP-LBD₁₀₅₆ in the absence and presence of potassium chromate and maltose. A) Thermal shift assays with MBP-LBD₀₉₈₇ in the absence or in the presence of 1 or 10 mM potassium chromate, or 10 mM maltose, are shown. B) Thermal shift assays with MBP-LBD₁₀₅₆ in the absence or in presence of 1mM or 10 mM potassium chromate are shown. Graphs represent the first derivative of the fluorescence emission ($-d(RFU)/dT$, RFU: Raw Fluorescence Unit) as a function of temperature. The melting temperatures (T_m) of each peak are listed in the tables to the right of each graph. Each graph is colored according to the tested ligand, as indicated. All graphs represent the results of three independent experiments.

We then performed TSAs to test chromate binding to both chimeric proteins. For MBP-LBD₀₉₈₇, neither 1 mM nor 10 mM chromate shifted the melt curve, and the T_m calculated for each moiety was not significantly modified (Fig. 3A). In contrast, for MBP-LBD₁₀₅₆, chromate modified its melting curve. Only the peak assigned to the LBD₁₀₅₆ moiety was altered, whereas the peak corresponding to MBP remained unaffected (Fig. 3B), signifying that the T_m associated with the MBP moiety remained

unchanged by chromate. The T_m that corresponded to the LBD₁₀₅₆ moiety increased significantly (2°C and 6.5°C in the presence of 1 mM and 10 mM chromate, respectively). A T_m shift of 2°C or more is considered significant and is a strong indicator of ligand binding [11,21,40,41].

Of the two chemoreceptors we identified as being involved in the chemotactic response to chromate, TSA indicated that one (SO_1056) directly binds chromate via its Cache-containing LBD. For the second chemoreceptor (SO_0987), no evidence of direct binding of chromate to the LBD was obtained. This finding indicates that either the chemoreceptor binds chromate via a different region of the protein, that chromate detection is indirect and requires an additional protein, or that for some unknown reason chromate binding to the LBD does not cause a significant shift in the melting temperature.

4. Conclusion

We previously developed a high-throughput technique to identify novel molecules that elicit a chemotactic response in bacteria [19]. Here, we propose a combination of efficient and simple protocols that can be used to assign chemotaxis-promoting compounds to chemoreceptors that bind their ligands directly. This approach can easily be scaled-up to perform high-throughput screening of chemoreceptors for a given ligand. As this is only a first step towards understanding signal detection, further characterization of the identified chemoreceptors must later be performed using more thorough biochemical techniques such as microscale thermophoresis, isothermal titration calorimetry, and structural analysis. The same approach could be used to identify the precise ligand-binding region after random mutagenesis of an LBD. Finally, these combined methods should be useful for biotechnology engineering, for example to design tools to detect pollutants.

Acknowledgments

We thank Marianne Ilbert, Amel Latifi and Baptiste Roumezi for their scientific and technical advices. We also thank Yann Denis from the Transcriptomic facility (IMM) for technical advices concerning TSAs. We thank all members of the group for their helpful discussions. We are also grateful to an anonymous reviewer whose suggestions helped improve and clarify this manuscript.

The authors acknowledge the funding from the Centre National de la Recherche Scientifique (www.cnrs.fr), Aix-Marseille Université (www.univ-amu.fr) and HTS-BIO (www.htsbio.com, Grant

345 N°152 660). A. B. was supported by a MESR fellowship and by an ATER position (Aix-Marseille
346 Université). The funders had no role in study design, data collection and interpretation, or the decision
347 to submit the work for publication.

348 The manuscript has been professionally proofread (Proof-Reading-Service.com).

349

350 AB, VM and CJC designed research. AB, AAC and CJC performed experiments. AB, AAC, VM and
351 CJC analyzed data. AB, VM and CJC wrote the manuscript.

352

353 The authors declare no conflict of interest.

354

355 **References**

- 356 [1] G.H. Wadhams, J.P. Armitage, Making sense of it all: bacterial chemotaxis, *Nat. Rev. Mol. Cell*
357 *Biol.* 5 (2004) 1024–1037. <https://doi.org/10.1038/nrm1524>.
- 358 [2] S. Bi, V. Sourjik, Stimulus sensing and signal processing in bacterial chemotaxis, *Curr. Opin.*
359 *Microbiol.* 45 (2018) 22–29. <https://doi.org/10.1016/j.mib.2018.02.002>.
- 360 [3] V. Sourjik, N.S. Wingreen, Responding to chemical gradients: bacterial chemotaxis, *Curr. Opin.*
361 *Cell Biol.* 24 (2012) 262–268. <https://doi.org/10.1016/j.ceb.2011.11.008>.
- 362 [4] A.I.M. Salah Ud-Din, A. Roujeinikova, Methyl-accepting chemotaxis proteins: a core sensing
363 element in prokaryotes and archaea, *Cell. Mol. Life Sci.* 74 (2017) 3293–3303.
364 <https://doi.org/10.1007/s00018-017-2514-0>.
- 365 [5] V.M. Gumerov, D.R. Ortega, O. Adebali, L.E. Ulrich, I.B. Zhulin, MiST 3.0: an updated
366 microbial signal transduction database with an emphasis on chemosensory systems, *Nucleic*
367 *Acids Res.* 48 (2020) D459–D464. <https://doi.org/10.1093/nar/gkz988>.
- 368 [6] R.P. Alexander, I.B. Zhulin, Evolutionary genomics reveals conserved structural determinants of
369 signaling and adaptation in microbial chemoreceptors, *Proc. Natl. Acad. Sci. U.S.A.* 104 (2007)
370 2885–2890. <https://doi.org/10.1073/pnas.0609359104>.
- 371 [7] J. Lacal, C. García-Fontana, F. Muñoz-Martínez, J.-L. Ramos, T. Krell, Sensing of environmental
372 signals: classification of chemoreceptors according to the size of their ligand binding regions,
373 *Environ. Microbiol.* 12 (2010) 2873–2884. <https://doi.org/10.1111/j.1462-2920.2010.02325.x>.

- 374 [8] V. Anantharaman, L. Aravind, Cache - a signaling domain common to animal Ca(2+)-channel
375 subunits and a class of prokaryotic chemotaxis receptors, Trends Biochem. Sci. 25 (2000) 535–
376 537. [https://doi.org/10.1016/s0968-0004\(00\)01672-8](https://doi.org/10.1016/s0968-0004(00)01672-8).
- 377 [9] A.A. Upadhyay, A.D. Fleetwood, O. Adebali, R.D. Finn, I.B. Zhulin, Cache Domains That are
378 Homologous to, but Different from PAS Domains Comprise the Largest Superfamily of
379 Extracellular Sensors in Prokaryotes, PLoS Comput. Biol. 12 (2016) e1004862.
380 <https://doi.org/10.1371/journal.pcbi.1004862>.
- 381 [10] Á. Ortega, I.B. Zhulin, T. Krell, Sensory Repertoire of Bacterial Chemoreceptors, Microbiol.
382 Mol. Biol. Rev. 81 (2017). <https://doi.org/10.1128/MMBR.00033-17>.
- 383 [11] A.F. Gasperotti, M.K. Herrera Seitz, R.S. Balmaceda, L.M. Prosa, K. Jung, C.A. Studdert, Direct
384 binding of benzoate derivatives to two chemoreceptors with Cache sensor domains in *Halomonas*
385 *titanicae* KHS3, Mol Microbiol. (2020). <https://doi.org/10.1111/mmi.14630>. Epub ahead of print.
386 PMID: 33098326.
- 387 [12] L.E. Ulrich, I.B. Zhulin, Four-helix bundle: a ubiquitous sensory module in prokaryotic signal
388 transduction, Bioinformatics. 21 Suppl 3 (2005) iii45-48.
389 <https://doi.org/10.1093/bioinformatics/bti1204>.
- 390 [13] J.T. Henry, S. Crosson, Ligand-binding PAS domains in a genomic, cellular, and structural
391 context, Annu. Rev. Microbiol. 65 (2011) 261–286. [https://doi.org/10.1146/annurev-micro-](https://doi.org/10.1146/annurev-micro-121809-151631)
392 [121809-151631](https://doi.org/10.1146/annurev-micro-121809-151631).
- 393 [14] J.S. Parkinson, G.L. Hazelbauer, J.J. Falke, Signaling and sensory adaptation in *Escherichia coli*
394 chemoreceptors: 2015 update, Trends Microbiol. 23 (2015) 257–266.
395 <https://doi.org/10.1016/j.tim.2015.03.003>.
- 396 [15] L.D. Miller, M.H. Russell, G. Alexandre, Diversity in bacterial chemotactic responses and niche
397 adaptation, Adv. Appl. Microbiol. 66 (2009) 53–75. [https://doi.org/10.1016/S0065-](https://doi.org/10.1016/S0065-2164(08)00803-4)
398 [2164\(08\)00803-4](https://doi.org/10.1016/S0065-2164(08)00803-4).
- 399 [16] J. Lacal, F. Muñoz-Martínez, J.-A. Reyes-Darías, E. Duque, M. Matilla, A. Segura, J.-J.O. Calvo,
400 C. Jiménez-Sánchez, T. Krell, J.L. Ramos, Bacterial chemotaxis towards aromatic hydrocarbons
401 in *Pseudomonas*, Environ. Microbiol. 13 (2011) 1733–1744. [https://doi.org/10.1111/j.1462-](https://doi.org/10.1111/j.1462-2920.2011.02493.x)
402 [2920.2011.02493.x](https://doi.org/10.1111/j.1462-2920.2011.02493.x).
- 403 [17] S. Bencharit, M.J. Ward, Chemotactic responses to metals and anaerobic electron acceptors in
404 *Shewanella oneidensis* MR-1, J. Bacteriol. 187 (2005) 5049–5053.
405 <https://doi.org/10.1128/JB.187.14.5049-5053.2005>.

- 406 [18] C. Baraquet, L. Théraulaz, C. Iobbi-Nivol, V. Méjean, C. Jourlin-Castelli, Unexpected
 407 chemoreceptors mediate energy taxis towards electron acceptors in *Shewanella oneidensis*, Mol.
 408 Microbiol. 73 (2009) 278–290. <https://doi.org/10.1111/j.1365-2958.2009.06770.x>.
- 409 [19] J. Armitano, C. Baraquet, V. Michotey, V. Méjean, C. Jourlin-Castelli, The chemical-in-μwell: a
 410 high-throughput technique for identifying solutes eliciting a chemotactic response in motile
 411 bacteria, Res. Microbiol. 162 (2011) 934–938. <https://doi.org/10.1016/j.resmic.2011.03.001>.
- 412 [20] M.K.G. Ehrhardt, S.L. Warring, M.L. Gerth, Screening Chemoreceptor-Ligand Interactions by
 413 High-Throughput Thermal-Shift Assays, Methods Mol. Biol. 1729 (2018) 281–290.
 414 https://doi.org/10.1007/978-1-4939-7577-8_22.
- 415 [21] M. Fernández, Á. Ortega, M. Rico-Jiménez, D. Martín-Mora, A. Daddaoua, M.A. Matilla, T.
 416 Krell, High-Throughput Screening to Identify Chemoreceptor Ligands, Methods Mol. Biol. 1729
 417 (2018) 291–301. https://doi.org/10.1007/978-1-4939-7577-8_23.
- 418 [22] A. Hida, T. Tajima, J. Kato, Two citrate chemoreceptors involved in chemotaxis to citrate and/or
 419 citrate-metal complexes in *Ralstonia pseudosolanacearum*, J. Biosci. Bioeng. 127 (2019) 169–
 420 175. <https://doi.org/10.1016/j.jbiosc.2018.07.014>.
- 421 [23] C. Bordi, C. Iobbi-Nivol, V. Méjean, J.-C. Patte, Effects of ISSo2 insertions in structural and
 422 regulatory genes of the trimethylamine oxide reductase of *Shewanella oneidensis*, J. Bacteriol.
 423 185 (2003) 2042–2045. <https://doi.org/10.1128/jb.185.6.2042-2045.2003>.
- 424 [24] M. Herrero, V. de Lorenzo, K.N. Timmis, Transposon vectors containing non-antibiotic
 425 resistance selection markers for cloning and stable chromosomal insertion of foreign genes in
 426 gram-negative bacteria., J Bacteriol. 172 (1990) 6557–6567.
 427 <https://doi.org/10.1128/jb.172.11.6557-6567.1990>.
- 428 [25] D.H. Figurski, D.R. Helinski, Replication of an origin-containing derivative of plasmid RK2
 429 dependent on a plasmid function provided *in trans*, Proc. Natl. Acad. Sci. U.S.A. 76 (1979) 1648–
 430 1652. <https://doi.org/10.1073/pnas.76.4.1648>.
- 431 [26] L.M. Guzman, D. Belin, M.J. Carson, J. Beckwith, Tight regulation, modulation, and high-level
 432 expression by vectors containing the arabinose PBAD promoter, J. Bacteriol. 177 (1995) 4121–
 433 4130. <https://doi.org/10.1128/jb.177.14.4121-4130.1995>.
- 434 [27] J. Armitano, V. Méjean, C. Jourlin-Castelli, Aerotaxis governs floating biofilm formation in
 435 *Shewanella oneidensis*, Environ. Microbiol. 15 (2013) 3108–3118. <https://doi.org/10.1111/1462-2920.12158>.
- 436
 437 [28] R.K. Appleyard, Segregation of New Lysogenic Types during Growth of a Doubly Lysogenic
 438 Strain Derived from *Escherichia coli* K12, Genetics. 39 (1954) 440–452. <https://doi.org/>

- 439 [29] C. Gambari, A. Boyeldieu, J. Armitano, V. Méjean, C. Jourlin-Castelli, Control of pellicle
 440 biogenesis involves the diguanylate cyclases PdgA and PdgB, the c-di-GMP binding protein
 441 MxdA and the chemotaxis response regulator CheY3 in *Shewanella oneidensis*, Environ.
 442 Microbiol. 21 (2019) 81–97. <https://doi.org/10.1111/1462-2920.14424>.
- 443 [30] H.S. Yu, M. Alam, An agarose-in-plug bridge method to study chemotaxis in the Archaeon
 444 *Halobacterium salinarum*, FEMS Microbiol. Lett. 156 (1997) 265–269.
 445 <https://doi.org/10.1111/j.1574-6968.1997.tb12738.x>.
- 446 [31] G. Vardar, P. Barbieri, T.K. Wood, Chemotaxis of *Pseudomonas stutzeri* OX1 and *Burkholderia*
 447 *cepacia* G4 toward chlorinated ethenes, Appl. Microbiol. Biotechnol. 66 (2005) 696–701.
 448 <https://doi.org/10.1007/s00253-004-1685-4>.
- 449 [32] K.D. Collins, T.M. Andermann, J. Draper, L. Sanders, S.M. Williams, C. Araghi, K.M.
 450 Ottemann, The *Helicobacter pylori* CZB Cytoplasmic Chemoreceptor TlpD Forms an
 451 Autonomous Polar Chemotaxis Signaling Complex That Mediates a Tactic Response to
 452 Oxidative Stress, J. Bacteriol. 198 (2016) 1563–1575. <https://doi.org/10.1128/JB.00071-16>.
- 453 [33] V. Korolik, K.M. Ottemann, Two Spatial Chemotaxis Assays: The Nutrient-Depleted
 454 Chemotaxis Assay and the Agarose-Plug-Bridge Assay, Methods Mol. Biol. 1729 (2018) 23–31.
 455 https://doi.org/10.1007/978-1-4939-7577-8_3.
- 456 [34] C. Roggo, E.E. Clerc, N. Hadadi, N. Carraro, R. Stocker, J.R. van der Meer, Heterologous
 457 Expression of *Pseudomonas putida* Methyl-Accepting Chemotaxis Proteins Yields *Escherichia*
 458 *coli* Cells Chemotactic to Aromatic Compounds, Appl. Environ. Microbiol. 84 (2018).
 459 <https://doi.org/10.1128/AEM.01362-18>.
- 460 [35] Y. Kalinin, S. Neumann, V. Sourjik, M. Wu, Responses of *Escherichia coli* bacteria to two
 461 opposing chemoattractant gradients depend on the chemoreceptor ratio, J. Bacteriol. 192 (2010)
 462 1796–1800. <https://doi.org/10.1128/JB.01507-09>.
- 463 [36] M.A. Machuca, A. Roujeinikova, Method for Efficient Refolding and Purification of
 464 Chemoreceptor Ligand Binding Domain, J Vis Exp. 130 (2017) 57092.
 465 <https://doi.org/10.3791/57092>.
- 466 [37] R.B. Kapust, D.S. Waugh, *Escherichia coli* maltose-binding protein is uncommonly effective at
 467 promoting the solubility of polypeptides to which it is fused, Protein Sci. 8 (1999) 1668–1674.
 468 <https://doi.org/10.1110/ps.8.8.1668>.
- 469 [38] S. Raran-Kurussi, D.S. Waugh, The ability to enhance the solubility of its fusion partners is an
 470 intrinsic property of maltose-binding protein but their folding is either spontaneous or chaperone-
 471 mediated, PLoS ONE. 7 (2012) e49589. <https://doi.org/10.1371/journal.pone.0049589>.

- [39] F.H. Niesen, H. Berglund, M. Vedadi, The use of differential scanning fluorimetry to detect ligand interactions that promote protein stability, *Nat Protoc.* 2 (2007) 2212–2221. <https://doi.org/10.1038/nprot.2007.321>.
- [40] D. Martín-Mora, A. Ortega, J.A. Reyes-Darias, V. García, D. López-Farfán, M.A. Matilla, T. Krell, Identification of a Chemoreceptor in *Pseudomonas aeruginosa* That Specifically Mediates Chemotaxis Toward α -Ketoglutarate, *Front Microbiol.* 7 (2016) 1937. <https://doi.org/10.3389/fmicb.2016.01937>.
- [41] J.L.O. McKellar, J.J. Minnell, M.L. Gerth, A high-throughput screen for ligand binding reveals the specificities of three amino acid chemoreceptors from *Pseudomonas syringae* pv. *actinidiae*, *Mol Microbiol.* 96 (2015) 694–707. <https://doi.org/10.1111/mmi.12964>.
- [42] H. Baaziz, C. Gambari, A. Boyeldieu, A. Ali Chaouche, R. Alatou, V. Méjean, C. Jourlin-Castelli, M. Fons, ChrASO, the chromate efflux pump of *Shewanella oneidensis*, improves chromate survival and reduction, *PLoS ONE.* 12 (2017) e0188516. <https://doi.org/10.1371/journal.pone.0188516>.

